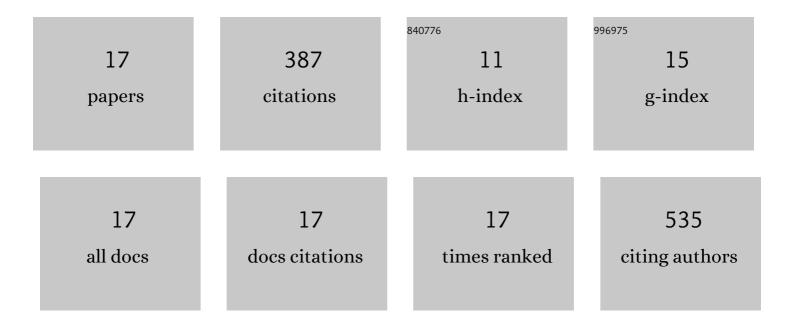
Ismail Cihan Kaya

List of Publications by Year in descending order

Source: https://exaly.com/author-pdf/7550815/publications.pdf Version: 2024-02-01



1 Production of CuOSE*WO3 hybrids and their dye removal capacity/performance from wastewater by adsorption/photocatalysis, Journal of Water Process Exprimeering, 2020, 36, 101390. 5.6 54 2 Efficient Vacuum-Deposited Perovskite Solar Cells with Stable Cubic. FA:SUB 184************************************	#	Article	IF	CITATIONS
2 FA:sub: 146* (15x:(f): (sub:) Adv.sub: (1x:(b): (sub:) PM:(sub:) 3:(sub:): ACS Energy Letters, 2020, 5; 3053:3061. 1.1/4 49 3 Interventional energy of the set of the set of the set of the set of set of set of the set of th	1	Production of CuO–WO3 hybrids and their dye removal capacity/performance from wastewater by adsorption/photocatalysis. Journal of Water Process Engineering, 2020, 36, 101390.	5.6	54
3 heterostructured photocatalysts for photocatalysts and phenolic pollutants. Materials Science 4.0 40 5 Photocatalysts degradation of organic dyes and phenolic pollutants. Materials Science 4.0 40 6 Highly efficient tandem photoelectrochemical solar cells using coumarin6 dye-sensitized CuCrO2 6.1 30 6 Highly efficient tandem photoelectrochemical solar cells using coumarin6 dye-sensitized CuCrO2 6.1 30 7 Stocab 2 (sub) canotibers. Journal of Appled Ceramic Technology. 2020, 17, 1479-1489. 21 23 8 Spray-Prolyced Tantalium-Doped TiO (sub) 2 (sub) 2 (sub) Compact Electron Transport Layer for UPP-processite Planar Perovskite Solar Cells Exceeding 20% Efficiency. ACS Appled Energy Materials, 2.2 20 9 Characteristics of Fe- and Mg-doped CuCrO2 nanocrystals prepared by hydrothermal synthesis. Journal of Materials Science. Materials in Electronic, 2016, 2.2, 2040-2411. 2.2 20 10 Vacumät@Apple.clean. Apple.clean. Advanced Energy and Sustainability Essa 2.1 21 10 Crystal Reorientation and Amorphization Induced by Stressing Efficient and Stable PaCHSC ^N 2.2	2	Efficient Vacuum-Deposited Perovskite Solar Cells with Stable Cubic FA _{1–<i>x</i>} MA _{<i>x</i>} Pbl ₃ . ACS Energy Letters, 2020, 5, 3053-3061.	17.4	49
4 high-efficiency photocatalytic degradation of organic dyes and phenolic pollutants. Materials Science 4.0 40 5 Photocatalytic extinty and delectric properties of hydrothermally derived tetragonal BaTiO3 nanoparticles using TiO2 nanofibers. Journal of Alloys and Compounds, 2018, 765, 82-91. 5.5 31 6 Highly efficient tandem photoelectrochemical solar cells using coumarin6 dye-sensitized CuCrO2 delafossite oxide as photocathode. Solar Energy, 2018, 169, 196-205. 6.1 30 7 Visible light active heterostructured photocatalyst system based on CuO plateaGike particles and SnO-sub22/sub nanofibers. International Journal of Applied Ceramic Technology, 2020, 17, 1479-1489. 2.1 28 8 UV-Photostabe/Enar Perovskite Solar Cells Exceeding 20% Efficiency. ACS Applied Energy Materials, 2022, 5, 3454-3462. 5.1 22 9 Characteristics of Fe- and Mg-doped CuCrO2 nanocrystals prepared by hydrothermal synthesis. 2021, 5, 3454-3462. 5.8 20 9 Characteristics of Fe- and Mg-doped CuCrO2 nanocrystals prepared by hydrothermal synthesis. 2.2 20 20 10 VaccumaRetrocesed MAPEL (sub 3 (slub) Perovskite Solar Cells. Advanced Energy and Sustainability Research, 2021, 2, 2000055. 5.8 20 11 honfact file of on hydrotalytic and delectric properties. International Journal of Applied Ceramic Technology, 2019, 16, 1557-1569. 11 10 <	3	heterostructured photocatalysts for photocatalytic applications. Dalton Transactions, 2018, 47,	3.3	46
3 nanoparticles using TiO2 nanofibers. Journal of Alloys and Compounds, 2018, 765, 82-91. 3-3 3-1 6 Highly efficient tandem photoelectrochemical solar cells using coumarin6 dye-sensitized CuCrO2 6.1 30 7 Shorsubs 2x/subs heterostructured photocatalyst system based on CuO plate36He particles and ShOrsubs 2x/subs nanofibers. International Journal of Applied Ceramic Technology, 2020, 17, 1479-1489. 2.1 23 8 Spray-Pyrolyzed Tantalium-Doped TiO (subs 2x/subs Compact Electron Transport Layer for UV-Photostable Planar Perovskite Solar Cells Exceeding 20% Efficiency. ACS Applied Energy Materials, 2022, 5, 3454-3462. 5.1 22 9 Characteristics of Fe- and Mg-doped CuCrO2 nanocrystals prepared by hydrothermal synthesis. 2022, 5, 3454-3462. 2.2 20 9 Characteristics of Fe- and Mg-doped CuCrO2 nanocrystals prepared by hydrothermal synthesis. 2022, 5, 3454-3462. 2.2 20 9 Characteristics of Fe- and Mg-doped CuCrO2 nanocrystals prepared by hydrothermal synthesis. 2022, 5, 3454-3462. 2.2 20 10 Crystal Reorientation and Amorphization Induced by Stressing Efficient and Stable PáC"IaC"N Vacuumãe Processed MAPDICsub-33(sub> Perovskite Solar Cells. Advanced Energy and Sustainability Research, 2021, 2, 2000065. 5.8 20 11 Crystal Reorientation and Amorphization Induced by Stressing Efficient and Stable PáC"IaC"N Vacuumãe Forecusal MAPDIcsub-34(sub-24/sub> nanoparticles usi	4	high-efficiency photocatalytic degradation of organic dyes and phenolic pollutants. Materials Science	4.0	40
6 delafossite oxide as photocathole. Solar Energy, 2018, 169, 196-205. 6-1 30 7 Visible light active heterostructured photocatalyst system based on CuO plate36lke particles and SnO _{2 2.1 23 8 Spray-Pyrolyzed Tantalium-Doped TiO₂ Compact Electron Transport Layer for UV-Photostable Planar Perovskite Solar Cells Exceeding 20% Efficiency. ACS Applied Energy Materials, 2022, 5, 3454-3462. 5.1 22 9 Characteristics of Fe- and Mg-doped CuCrO2 nanocrystals prepared by hydrothermal synthesis. 2022, 5, 3454-3462. 2.0 20 10 Crystal Reorientation and Amorphization Induced by Stressing Efficient and Stable Pa6"lä6"N Vacuumä6Processed MAPbl(sub>3} Perovskite Solar Cells. Advanced Energy and Sustainability Research, 2021, 2, 2000065. 5.8 20 11 nanofibers: Study on photocatalytic and dielectric properties. International Journal of Applied Ceramic Technology, 2019, 16, 1557-1569. 2.1 15 12 transporting layer for highly stable perovskite solar cells with efficiency over 22%. Journal of Materials Chemistry A, 2022, 10, 12464-12472. 13 14 13 Intrinsic Organic Semiconductors as Hole Transport Layers in på6"lä6"n Perovskite Solar cells. Solar Rrl, 2022, 6, . 5.8 8 14 Enamine-based hole transporting materials for vacuum-deposited perovskite solar cells. Sustainable Energy and Fuels, 2022, 4, 5017-5023. 5.8 8	5	Photocatalytic activity and dielectric properties of hydrothermally derived tetragonal BaTiO3 nanoparticles using TiO2 nanofibers. Journal of Alloys and Compounds, 2018, 765, 82-91.	5.5	31
7 SnO-sub3-2 nanofibers. International journal of Applied Ceramic Technology, 2020, 17, 1479-1489. 2.1 23 8 Spray-Pyrolyzed Tantalium-Doped TIO <sub3-2< td=""> Sopray-Pyrolyzed Tantalium-Doped TIO<sub3-2< td=""> Sopray-Pyrolyzed Tantalium-Doped TIO Sopray-Pyrolyzed Tantalium-Doped TopeTion Sopray-Pyrolyzed Tantalium-DopeTion Sopray-Pyrolyzed Tantantalium-Doped Toperation So</sub3-2<></sub3-2<></sub3-2<></sub3-2<></sub3-2<></sub3-2<></sub3-2<></sub3-2<>	6	Highly efficient tandem photoelectrochemical solar cells using coumarin6 dye-sensitized CuCrO2 delafossite oxide as photocathode. Solar Energy, 2018, 169, 196-205.	6.1	30
8 LV-Photostable Planar Perovskite Solar Cells Exceeding 20% Efficiency. ACS Applied Energy Materials, 2022, 5, 3454-3462. 5.1 22 9 Characteristics of Fe- and Mg-doped CuCrO2 nanocrystals prepared by hydrothermal synthesis. Journal of Materials Science: Materials in Electronics, 2016, 27, 2404-2411. 2.2 20 10 Vacumãe Processed MAPble sub 3 Sub 2016, 27, 2404-2411. 5.8 20 10 Vacumãe Processed MAPble sub 3 Sub 2 Sub 2 Sub 2 Sub 2 10 Vacumãe Processed MAPble sub 3 Sub 3 <	7		2.1	23
9 Journal of Materials Science: Materials in Electronics, 2016, 27, 2404-2411. 2.22 20 10 Crystal Reorientation and Amorphization Induced by Stressing Efficient and Stable PäC"IäC"N VacuumäEProcessed MAPbl (sub>3 Perovskite Solar Cells. Advanced Energy and Sustainability Research, 2021, 2, 2000065. 5.8 20 11 Hydrothermal synthesis of pseudocubic BaTiO (sub>3 nanoparticles using TiO (sub>2 nanofibers: Study on photocatalytic and dielectric properties. International Journal of Applied 2.1 15 12 Adopant-free 2,7-diocty[1][benzothion[3,2-(i)bc/i>[1][benzothiophene (C8-BTBT)-based hole transporting layer for highly stable perovskite solar cells with efficiency over 22%. Journal of Materials Chemistry A, 2022, 10, 12464-12472. 10.3 14 13 Intrinsic Organic Semiconductors as Hole Transport Layers in päC"iaC"n Perovskite Solar Cells. Solar Rrl, 2022, 6, . 5.8 8 14 Enamine-based hole transporting materials for vacuum-deposited perovskite solar cells. Sustainable Energy and Fuels, 2020, 4, 5017-5023. 4.9 6 15 Future perspectives of perovskite solar cells: Metal oxide-based inorganic hole-transporting materials., 2021, 1, 181-219. 5 16 Production and Characterization of MagnesiumäEDoped Copper Chromite Fibers. Physica Status Solidi (A) Applications and Materials Science, 2018, 215, 1700795. 1.8 4	8	UV-Photostable Planar Perovskite Solar Cells Exceeding 20% Efficiency. ACS Applied Energy Materials,	5.1	22
10 Vacuumâ¢Processed MAPbl ₃ Perovskite Solar Cells. Advanced Energy and Sustainability Research, 2021, 2, 2000065. 5.8 20 11 Hydrothermal synthesis of pseudocubic BaTiO ₃ nanoparticles using TiO ₂ 2.1 15 11 ceramic Technology, 2019, 16, 1557-1569. 2.1 15 12 A dopant-free 2,7-dioctyl[1]benzothien0[3,2- <i>><i>><i>><i>><i>><i>><i>><i>><i> 10.3 14 13 Intrinsic Organic Semiconductors as Hole Transport Layers in på€"iâ€"n Perovskite Solar Cells. Solar Rrl, 2022, 6, . 5.8 8 14 Enamine-based hole transporting materials for vacuum-deposited perovskite solar cells. Sustainable Lerergy and Fuels, 2020, 4, 5017-5023. 6.8 8 15 Future perspectives of perovskite solar cells: Metal oxide-based inorganic hole-transporting materials ., 2021, 181-219. 5 16 Production and Characterization of Magnesiumã€Doped Copper Chromite Fibers. Physica Status Solidi (A) Applications and Materials Science, 2018, 215, 1700795. 1.8 4</i></i></i></i></i></i></i></i></i>	9	Characteristics of Fe- and Mg-doped CuCrO2 nanocrystals prepared by hydrothermal synthesis. Journal of Materials Science: Materials in Electronics, 2016, 27, 2404-2411.	2.2	20
11 nanofibers: Study on photocatalytic and dielectric properties. International Journal of Applied 2.1 15 12 A dopant-free 2,7-dioctyl[1]benzothieno[3,2- <i>b</i> [1]benzothiophene (C8-BTBT)-based hole 10.3 14 12 transporting layer for highly stable perovskite solar cells with efficiency over 22%. Journal of 10.3 14 13 Intrinsic Organic Semiconductors as Hole Transport Layers in p–i–n Perovskite Solar Cells. Solar Rrl, 5.8 8 14 Enamine-based hole transporting materials for vacuum-deposited perovskite solar cells. Sustainable 4.9 6 15 Future perspectives of perovskite solar cells: Metal oxide-based inorganic hole-transporting materials. 2021, 181-219. 5 16 Production and Characterization of Magnesium Doped Copper Chromite Fibers. Physica Status Solidi 1.8 4 16 EARRICATION OF THE P-N IUNCTION ULTRAVIOI ET PHOTODETECTORS BASED ON METAL OXIDE 1.8 4	10	Vacuumâ€Processed MAPbl ₃ Perovskite Solar Cells. Advanced Energy and Sustainability	5.8	20
12 transporting layer for highly stable perovskite solar cells with efficiency over 22%. Journal of 10.3 14 13 Intrinsic Organic Semiconductors as Hole Transport Layers in p–i–n Perovskite Solar Cells. Solar Rrl, 2022, 6, . 5.8 8 14 Enamine-based hole transporting materials for vacuum-deposited perovskite solar cells. Sustainable Energy and Fuels, 2020, 4, 5017-5023. 4.9 6 15 Future perspectives of perovskite solar cells: Metal oxide-based inorganic hole-transporting materials. , 2021, , 181-219. 5 16 Production and Characterization of Magnesiumâ€Doped Copper Chromite Fibers. Physica Status Solidi (A) Applications and Materials Science, 2018, 215, 1700795. 1.8 4	11	nanofibers: Study on photocatalytic and dielectric properties. International Journal of Applied	2.1	15
13 2022, 6, . 5.8 8 14 Enamine-based hole transporting materials for vacuum-deposited perovskite solar cells. Sustainable 4.9 6 14 Energy and Fuels, 2020, 4, 5017-5023. 4.9 6 15 Future perspectives of perovskite solar cells: Metal oxide-based inorganic hole-transporting materials. , 2021, , 181-219. 5 16 Production and Characterization of Magnesiumâ€Doped Copper Chromite Fibers. Physica Status Solidi 1.8 4 EABRICATION OF THE P-N IUNCTION ULTRAVIOLET PHOTODETECTORS BASED ON METAL OXIDE	12	transporting layer for highly stable perovskite solar cells with efficiency over 22%. Journal of	10.3	14
14 Energy and Fuels, 2020, 4, 5017-5023. 4.9 6 15 Future perspectives of perovskite solar cells: Metal oxide-based inorganic hole-transporting 5 16 Production and Characterization of Magnesiumâ€Doped Copper Chromite Fibers. Physica Status Solidi 1.8 4 16 FABRICATION OF THE P-N IUNCTION ULTRAVIOLET PHOTODETECTORS BASED ON METAL OXIDE 1.8 4	13		5.8	8
 materials., 2021, , 181-219. Production and Characterization of Magnesiumâ€Doped Copper Chromite Fibers. Physica Status Solidi 1.8 4 FABRICATION OF THE P-N IUNCTION ULTRAVIOLET PHOTODETECTORS BASED ON METAL OXIDE 	14		4.9	6
(A) Applications and Materials Science, 2018, 215, 1700795.	15			5
FABRICATION OF THE P-N JUNCTION UI TRAVIOI ET PHOTODETECTORS BASED ON METAL OXIDE	16	Production and Characterization of Magnesiumâ€Doped Copper Chromite Fibers. Physica Status Solidi (A) Applications and Materials Science, 2018, 215, 1700795.	1.8	4
¹⁷ NANOPARTICLES. Konya Journal of Engineering Sciences, 2022, 10, .	17	FABRICATION OF THE P-N JUNCTION ULTRAVIOLET PHOTODETECTORS BASED ON METAL OXIDE NANOPARTICLES. Konya Journal of Engineering Sciences, 2022, 10, .	0.3	0